Integrating Shape and Texture for Hand Verification

Ajay Kumar, David Zhang
Department of Computing,
The Hong Kong Polytechnic University
Kowloon, Hong Kong.
Email: *ajaykr@ieee.org*, *csdzhang@comp.polyu.edu.hk*

Abstract: *This paper investigates the performance of a bimodal biometric system using fusion of shape and texture. We propose several new hand shape features that can be used to represent the hand shape and improve the performance for hand shape based user authentication. We also demonstrate the usefulness of Discrete Cosine Transform* (*DCT*) *coefficients for palmprint authentication. The score level fusion of hand shape and palmprint features using product rule achieves best performance as compared to Max or Sum rule. However the decisions from the Sum, Max, and Product rules can also be combined to further enhance the performance. Thus the fusion of score level decisions, from the multiple strategies, is proposed and investigated. The two hand shapes of an individual are anatomically similar. However, the palmprints from two hands can be combined to further improve performance and is demonstrated in this paper.*

1. Introduction

The increasing demand for automated personal identification has led to an unprecedented interest in biometrics. Traditional methods of personal identification, *i.e.* passports, ID cards or passwords, can be forgotten or lost and are prone to planned fraudulent attacks. A recent study [1] has revealed that about 40-80% IT help desk calls are attributed to forgotten passwords and at NY times website about 1000 people per week forget their passwords. The physiological or behavioral characteristics of humans, *i.e.* biometrics, are highly stable, unique and universal for their usage in automated personal authentication. However, the performance of current biometric based personal authentication systems has not yet matured for their (reliable usage)/deployment in real environment.

The Primary objective of any biometric authentication system [2] is to achieve higher performance while utilizing most of the discriminant features. The human hand is rich stimulus that provides diverse and unique information to identify an individual. The fingerprint, palmprint and hand-shape can be simultaneously extracted from a typical human hand image. However the nature of features (minutiae) traditionally employed for the fingerprint matching requires a high resolution fingerprint image which is several times higher than those required for palmprint or hand-shape. The hand images of such high resolution will require complex imaging setup, higher memory for storage and retrieval, and large computational power for online verification. However the acquisition of hand images that can deliver palmprint and hand-shape information is easy and has been demonstrated in [3]. In the context of recent work in [3] and the current popularity of multimodal system, this assertion that palmprint could offer improved performance while integrating with hand shape, deserves careful evaluation. The experiments reported in this paper are aimed at: (i) improving the performance of hand-shape authentication by exploring new features, (ii) investigating the palmprint authentication in frequency domain using popular

DCT coefficients, (iii) investigating the performance improvement when the palmprint images from both the hands are combined, and (iv) examining the possibility of combining multiple decisions from the multiple fusion strategies at score level to achieve performance improvement.

1.1 Prior Work

Personal authentication using hand-shape features has shown promising results in the literature [4]-[7]. The methods proposed in [4]-[6] use signature analysis on the binary hand-shape boundary image to extract various geometric features. However, the performance analysis of these methods has been evaluated on small size database which was acquired in constrained conditions using fixation-pegs to restrict the feature variance due to rotation and translation. Recently, Oden *et al*. [7] investigated the fusion of algebraic invariants from the implicit polynomials and geometric shape features for hand recognition. However, their performance evaluation on small size database of 35 users is not sufficient to make any reliable conclusion. The usage of palmprint images for online user authentication using Gabor phase features has been illustrated in [8]. Zhang and Shu [9] have proposed that the location and orientation of major palmprint lines can be used to identify palmprints. The palmprint recognition using *PalmCode* representation has been proposed in [10]. Prior work [8] on online palmprint authentication used the palmprint images acquired using fixation pegs which was useful to restrict the feature variance due to translation and rotation of hands on image sensor. However, the images acquired from peg-free imaging setup [3] have higher user-acceptance and has been used in this work.

1.2 Proposed System

The block diagram of the hand-based authentication system is shown in Figure 1. The hand images acquired from the digital camera are used to extract two distinct images: (i) binary image depicting hand-shape, and (ii) gray-level region of interest (ROI) depicting palmprint texture.

The method of extracting these two images is same as reported in earlier study [3]. Each of the extracted binary hand-shape image is further processed with morphological operations to remove any isolated small blobs or holes. The details of features extracted from hand-shape and palmprint images are in following two sections

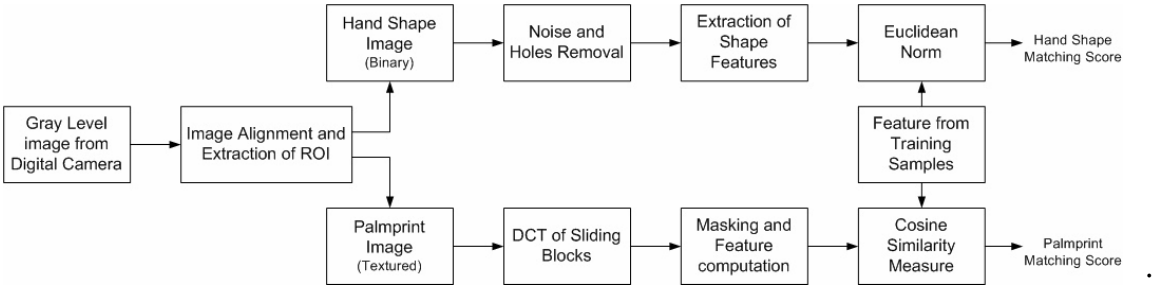

Figure 1: Block diagram of experimental setup for personal authentication using hand images.

2. Hand-Shape Matching

Hand-shape representation requires effective and perceptually important features based on geometrical information or geometry plus interior content. Shape is an important visual feature and has been used to describe and retrieve the image content [11],[13]. There are several properties, *i.e.* perimeter, solidity, extent, eccentricity, position of centroid relative to shape boundary, convex area, that have been used to characterize and describe a shape. We investigate the usefulness of these shape properties to characterize the hand-shape. The solidity of hand-shape is computed as the ratio between the hand area and the area corresponding to convex hull. The extent of hand-shape is measured by hand area divided by the area of minimum bounding rectangle (smallest rectangle that totally encloses the hand-shape). The parameters of best-fitting ellipse were computed using the method of moments [14] and used to compute the eccentricity, *i.e.*, ratio of minor axis length to major axis length. Further definition and details of extracting these shape features can be found in references [12]-[14]. Thus a hand-shape can be better described by a set of 23 features; 4 finger length, 8 finger width, palm-width, palm-length, hand-area, and hand-length (as detailed in [3]) and seven shape measures described earlier. The feature

vectors from hand-shape image for every user is computed and stored during user enrollment. The distance between feature vector from an unknown hand-shape f and that from the known class j is computed from the Euclidean norm ($\|.\|$), *i.e.*,

$$h(f, f_j) = \sum_i \left| f^i - f_j^i \right| \tag{1}$$

The performance for user authentication is ascertained using receiver operating characteristics from the test samples. The performance improvement due to the usage of 23 features, as compared to 16 features in [3], can be observed from Figure 2 (b). The palmprint matching score is consolidated with the distance measure $h(f, f_j)$ and this is discussed in section 4.

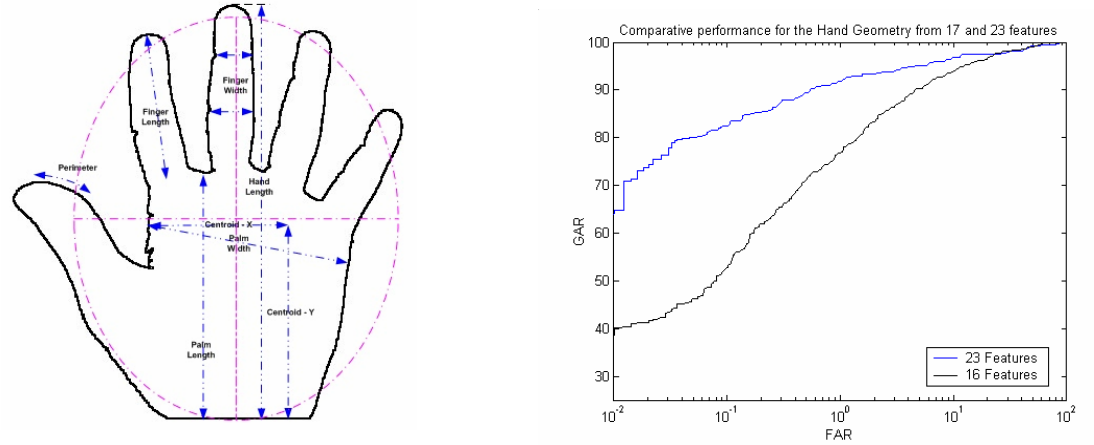

(a) (b)

Figure 2: (a) Some of the hand shape features extracted from the binary image; (b) Comparative receiver operating characteristics for the two cases to ascertain the performance.

3. Palmprint Matching

The palmprint matching using texture-based [8], [10], line-based, [9], and appearance based methods [15] have been proposed literature. The spatial-frequency domain features are less sensitive to noise and intensity variations than those features from spatial domain. The Discrete Cosine Transform (DCT) has become one of the most successful transforms in image processing for the purpose of data compression, feature extraction, and recognition. The computational efficiency of the statistically sub-optimal transform is very high due to the various kind of fast

algorithms [16] developed. However the significance of DCT for palmprint images is yet to be investigated. The DCT that maps a $P \times Q$ spatial image block $I(p,q)$ to its values in frequency domain can be defined as follows:

$$\Omega(x,y) = \sum_{p=0}^{P-1}\sum_{q=0}^{Q-1} 4I(p,q)\cos\frac{\pi(2p+1)x}{2P}\cos\frac{\pi(2q+1)y}{2Q} \tag{2}$$

The palmprint image is divided into overlapping blocks of $P \times Q$ pixels size and the DCT coefficients, *i.e.* $\Omega(x,y)$, for each of these blocks is computed. Several of these DCT coefficients have values close to zero and can be discarded. In this work, all of the block DCT coefficients except those shown in Figure 3 are discarded. The feature vector from palmprint image is formed by computing standard deviation of these significant DCT coefficients in each of these overlapping blocks.

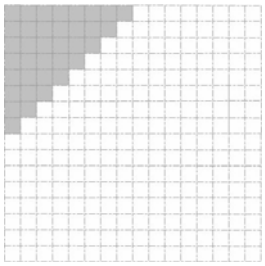

Figure 3: Mask used to compute significant DCT coefficients from each of the 324 blocks.

The cosine similarity measure is used to compute the distance between the feature vector f and that from unknown class j;

$$p(f,f_j) = 1 - \frac{f^T.f_j}{\|f\|.\|f_j\|} \tag{3}$$

While matching the unknown feature vector f_j with the ones from the training samples, the maximum of similarity measure is assigned as the final matching distance

4. Fusion Strategies

The score level fusion that can consolidate the matching scores from multiple evidences has shown [17]-[18] to offer radical increase in performance and has been the focus of our experiments. We investigated the performance of Sum, Max, and Product rules on the matching scores from the palmprint and hand-shape. It was observed that the performance of these three fusion strategies gives different results. Therefore judicious combination of matching scores has been investigated to achieve the performance improvement. The palmprint matching scores from the two hands can be used to further enhance the performance at score level. Thus the palmprint matching scores from the two hands, *i.e*. left and right hand, are consolidated by using Sum rule. These consolidated matching scores are further combined with those from the hand-shape using Product rule, as shown in the Figure 4 [19]. Thus in two distinct scenarios, *i.e*. users are asked to present one or two hands, we employ two separate fusion strategies to achieve the performance improvement.

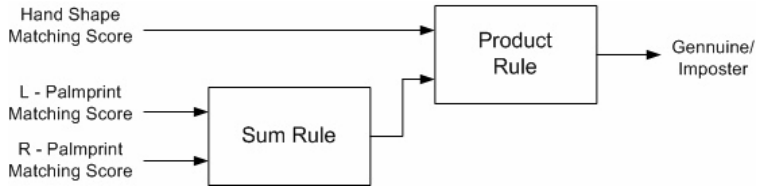

Figure 4: Combining right and left palmprint matching scores with those from hand-shape.

5. Experiments and Results

In order to examine the goals of our experiments the image database from 100 users was employed. The image acquisition setup using a digital camera was employed to collect 10 images per user. These hand images were collected during an average period of three month, as the goal of experiments was to investigate the fusion of biometric modalities instead of their stability with time. The preprocessing described in earlier study [3] was used to obtain palmprint and hand-shape images. The size of each of the segmented gray-level palmprint image was 300 ×

300 pixels. Each of these images were divided into 16 × 16 pixels with an overlapping of 6 pixels. The extent of this overlapping distance was determined from the experiments; the overlapping distance was varied from 0-8 pixels (50%) and the overlapping distance with best performance was employed for further experiments. The feature vector of size 1 × 23 from hand-shape image and 1 × 324 from the palmprint image was used to evaluate the performance. We employed five image samples from every user for training and the rest five images for the testing the performance.

Hand Image	Extent	Eccentricity	Solidity
	0.51	0.74	0.71
	0.63	0.78	0.80
	0.47	0.65	0.69
	0.53	0.69	0.73
	0.58	0.76	0.77
	0.47	0.74	0.65

Figure 5: Some hand-shape images and their corresponding extent, eccentricity, and solidity values.

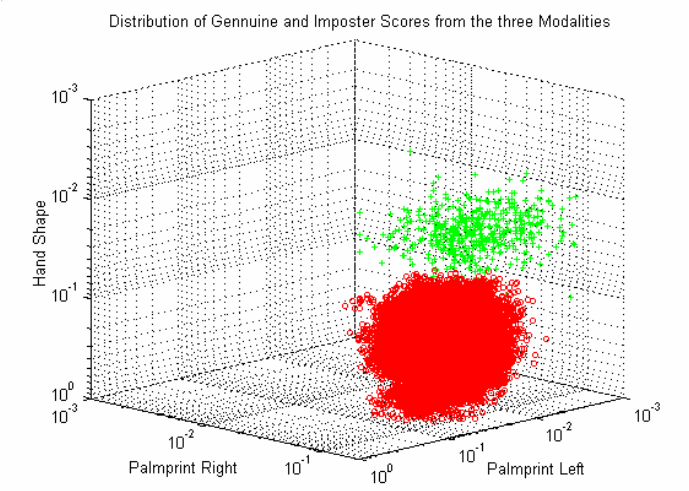

Figure 6: The distribution of genuine and imposter matching scores from the hand-shape and palmprints.

Some of the hand-shape images from our database along with their extent, eccentricity, and solidity values are shown in Figure 5. Figure 6 shows the genuine and imposter distribution of test data from the hand-shape and both of the palmprints. The hand-shape was only extracted from the left hand images and the fusion results with left palmprint are displayed in Figure 7. The receiver operating characteristics (ROC) shows that the product rule achieves best performance as compared to those from Sum or Max rule. The individual ROC for hand-shape, left and right palmprint is shown in Figure 8. In order to ascertain the comparative performance, the combined ROC from hand-shape, left and right palmprint, using fusion scheme in Figure 4, is also shown. Thus the performance improvement due to the usage of right palmprint with the left palmprint and hand-shape can be visualized from Figure 8. The quantitative performance corresponding to each of the case in Figure 8 is shown in Table 1. The parameters of total minimum error, along with their respective decision threshold and Equal Error Rate (*EER*) are displayed in this Table. The performance score from each of these cases can also be ascertained by objective function J [11];

$$J = \frac{(\mu_g - \mu_i)^2}{\sigma_g^2 + \sigma_i^2} \tag{4}$$

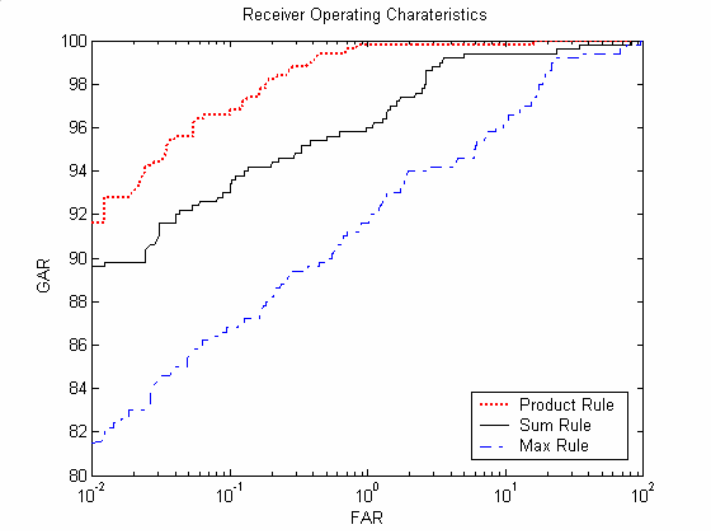

Figure 7: The comparative ROC for the hand-shape and left palmprint using three fusion rules

where μ_g, μ_i are the mean and σ_g, σ_i are the standard deviation of genuine and impostor distributions respectively. The genuine and imposter distributions for each of the cases in Figure 8 are displayed in Figure 9 and their corresponding performance indices, *i.e.* J, is displayed in Table 1. It can be noticed from Figure 9 that the separation of genuine and imposter distributions has improved with the integration of palmprint features in Figure 9 (d) and (e). The significant reduction in error rates, *i.e.* total minimum error, as compared to those achieved by hand-shape or palmprint alone can be observed from the entries in Table 1.

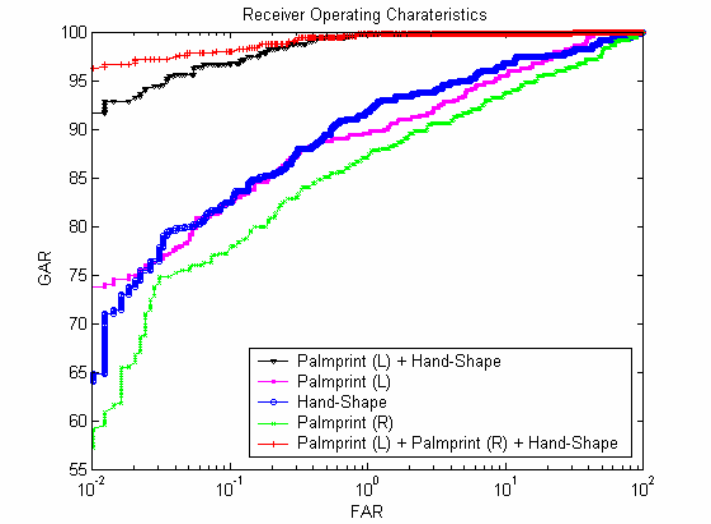

Figure 8: The comparative ROC from the hand-shape and palmprints in the experiments.

Table 1: Performance Indices for Individual Modalities and Fusion from Matching Scores.

Modalities	Total Minimum Error				
	FAR	*FRR*	Threshold	*EER*	*J*
Hand-Shape	1.57	6.60	0.0806	5.00	2.55
Palmprint – L	0.89	10.0	0.0129	6.00	2.48
Palmprint –R	2.94	9.40	0.0423	7.10	3.45
Hand-Shape + Palmprint – L	0.43	0.60	0.0284	0.60	4.88
Hand-Shape + Palmprint – (L+R)	0.32	0.60	0.0477	0.60	6.18

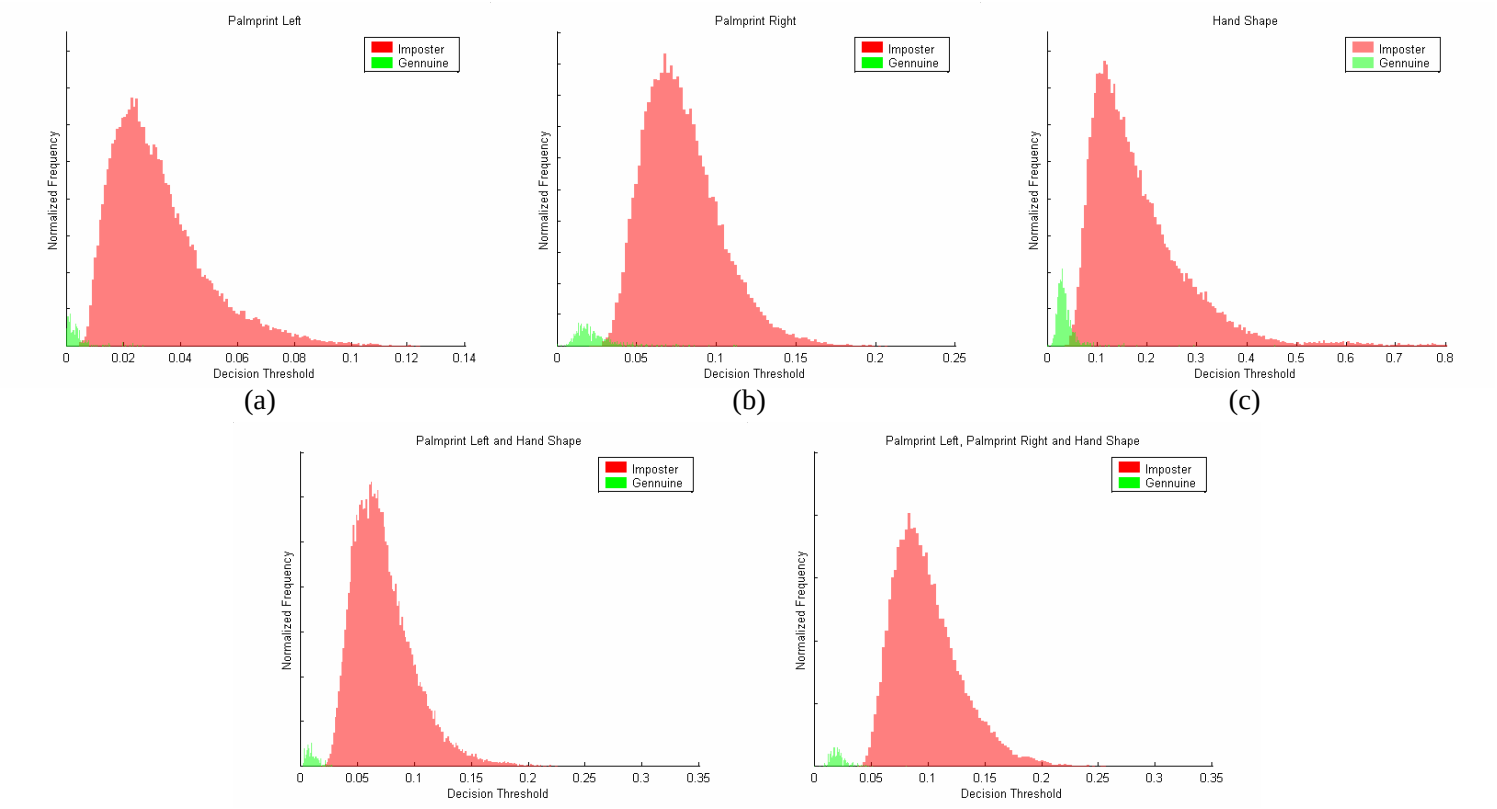

Figure 9: The scaled cumulative distribution of genuine and imposter scores from the (a) Left Palmprint, (b) Right Palmprint, (c) Hand Shape, (d) Fusion Hand Shape and Left Palmprint, (e) Fusion of both Palmprints and Hand Shape.

6. Summary and Conclusions

Our experimental results in Figure 2 suggested the usefulness of shape properties, *e.g*. perimeter, extent, solidity, centroid, investigated for the hand-shape authentication. Similarly our approach for palmprint matching using DCT coefficients has also shown promising results. This

investigation is useful as the DCT coefficients can be directly obtained from the camera hardware using commercially available DCT chips that can perform fast and efficient DCT transforms. The fusion of palmprint and hand-shape matching scores has been useful to achieve higher performance, which is also the conclusion from earlier study [3]. However, using more promising features, matching criterion, and more rigorous assurance from the simple fusion strategies, we obtained better results than in earlier study. More importantly, the fusion strategy employed in Figure 4 can also be used in the fusion of other biometric modalities to achieve higher performance.

The hand-shape information from the two hands of a healthy individual is anatomically similar. Despite the similarity of major principal lines in the two palmprint of an individual, the detailed palmprint texture from an individual are different, and thus the palmprint information from the other hand can also be used to enhance the confidence in authentication. Therefore this paper has also investigated the performance enhancement (Table 1) with the integration of palmprint information from the both hands and the hand-shape. However, the performance enhancement using the palmprint information from other hand may not be justifiable due to the increase in the user inconvenience and the cost of the system. The integration of fingerprint features from the same hand, along with palmprint and hand-shape features, can certainly offer better alternative and such a system is suggested for future work.

7. References

[1] Gartner, Inc., http://www.gartner.com

[2] D. Zhang (*Ed.*), *Biometrics Solutions for Authentication in an e-World*, Kluwer Academic Publishers, USA, 2002

[3] A. Kumar, D. C. M. Wong, H. Shen, and A. K. Jain, "Personal verification using palmprint and hand geometry biometric," *Proc. AVBPA*, pp. 668-675, June 2003.

[4] A. K. Jain, A. Ross, and S. Pankanti, "A Prototype hand geometry-based verification system, *Proc. AVBPA*, pp. 166-171, Washington, DC, USA, 1999.

[5] R. L. Zunkei, Hand geometry based verification; A. K. Jain, R. Bollen, and S. Pankanti (Eds), *Biometrics: Personal identification in networked society*, Kluwer Academic, Dordrecht, pp. 87-101, 1999.

[6] R. Sanchez-Reillo, C. Sanchez-Avila, A. Gonzales-Marcos, "Biometric identification through hand geometry measurements," *IEEE Trans. Patt. Anal. Machine Intell.*, vol. 22, pp. 1168-1171, Oct. 2000.

[7] C. Oden, A. Ercil, and B. Buke, "Combining implicit polynomials and geometric features for hand recognition," *Pattern Recognition Letters*, vol. 24, pp. 2145-2152, 2003.

[8] D. Zhang, W.K. Kong, J. You, and M. Wong, "On-line palmprint identification," *IEEE Trans. Patt. Anal. Machine Intell.*, vol. 25, pp. 1041-1050, Sep. 2003.

[9] D. Zhang and W. Shu, "Two novel characteristics in palmprint verification: datum point invariance and line feature matching," *Pattern Recognit*ion, vol. 32, no. 4, pp. 691-702, Apr. 1999.

[10] A, Kumar and H. C. Shen, "Palmprint Identification Using PalmCodes," *Proc*. *Intl. Conf. Image & Graphics*, *ICIG 2004*, pp. 258-261, Hong Kong, Dec. 2004.

[11] D. Zhang and G. Lu, "Review of shape representation and description techniques," *Pattern Recognition*, vol. 37, pp. 1-19, 2004.

[12] John C. Russ, *The Image Processing Handbook*, 3rd ed., CRC Press, Boca Eaton, Florida, 1999.

[13] O. El. Badawy and M. Kamel, "Shape-based image retrieval applied to trademark images," *Int. J. Image & Graphics*, vol. 2, no. 3, pp. 375-393, 2002.

[14] R. M. Haralick and L. G. Shapiro, *Computer Vision and Robot Vision*, Addison-Wesley, 1991.

[15] A, Kumar and H. C. Shen, "Recognition of palmprints using eigenpalms," *Proc. CVRIP 2003*, Cary (North Carolina), USA, Sep. 2003.

[16] Z. Wang, Z. He, C. Zou, and J. D. Z. Chen, "A generalized fast algorithm for n-D discrete cosine transform and its application to motion picture coding*," IEEE Trans. Circuits & Sys., Part II*, Vol. 46, May 1999.

[17] S. Prabhakar and A. K. Jain, "Decision level fusion in fingerprint verification," *Pattern Recognition*, vol. 35, pp. 861-874, 2002.

[18] A. Kumar and D. Zhang, “Integrating palmprint with face for user authentication,” *Proc. Multi Modal User Authentication Workshop*, pp. 107-112, Santa Barbara, CA, USA, Dec. 11-12, 2003

[19] A. Kumar and D. Zhang, “Palmprint authentication using multiple classifiers,” *Proc. SPIE Symposium- Biometric Technology for Human Identification*, Vol. 5404, pp. 20-29, Orlando, FL, USA, Apr.12-13, 2004.